Progress of Theoretical Physics, Vol. 102, No. 1, July 1999

Hierarchical Structure of Astronomical Objects in the Cosmic String Scheme

Tetsuya HARA, Petri MÄHÖNEN,* Toru HIRAYAMA and Shigeru J. MIYOSHI

Department of Physics, Kyoto Sangyo University, Kyoto 603-8555, Japan
**Department of Theoretical Physics, University of Oulu, SF-90570 Oulu, Finland*

(Received March 25, 1998)

The hierarchical structure of astronomical objects is investigated in the cosmic string scheme with cold dark matter (CDM). A non-linear dark matter potential is formed in the crossing site of three wakes triggered at around $z_{\rm i}$ by moving strings. If we use this scheme, the mass and radius of formed CDM objects increase gradually as $M \propto (1+z)^{-3}$ and $R \propto (1+z)^{-2}$, and objects triggered at $z_{\rm i} \simeq 10^4$, 10^5 and 10^6 grow to become objects corresponding to clusters of galaxies, galaxies and dwarf galaxies, respectively. The number densities of these objects $n(z_{\rm i})$ are related to the size $l(z_{\rm i}, z)$ as $n(z_{\rm i}) \propto 1/l(z_{\rm i}, z)^3$, where $l(z_{\rm i}, z)$ is the horizon size of the stage $z_{\rm i}$ observed at z.

One of the interesting points of this scheme is that smaller objects are gradually accreted into larger ones. For example, dwarf galaxies have been mostly accreted into galaxies at the present. Galaxies are still now accumulating toward clusters of galaxies, and consequently many of accreted galaxies are found as E or SO type galaxies there. In the future, or possibly even at the present time, clusters of galaxies will be accreted into superclusters of galaxies triggered at $z_{\rm i} \simeq 10^3$.

Heating through the accumulation of baryonic matter in the CDM gravitational potential is also investigated and it is found that their heating is not sufficient to reionize the universe before $z \simeq 5$. Therefore some other heating sources or mechanisms are required. However, heating through the accumulation of baryonic matter could explain the X-ray properties of clusters of galaxies.

§1. Introduction

A hierarchical structure of astronomical objects, e.g. clusters of galaxies, galaxies, dwarf galaxies and globular clusters has been observed. With the exception of globular clusters, these objects are thought to form through the increase of the initial fluctuations of cold dark matter (CDM) and later through clustering. There are many works on the formation of these astronomical objects in the standard CDM scheme,[1] assuming a power spectrum of random Gaussian initial fluctuations. The validity of this scheme has been extensively investigated.[2] Here, we attempt to solve the problem in the non-Gaussian spectrum, e.g. within the cosmic string scheme,[3),4] considering the hierarchical structure of astronomical objects.

It has been said that string network simulations are not consistent with the observation in small angle anisotropies.[5] However, there are some assumptions in these simulations[5),6] and uncertainties in the observations. Recently it has been reported that local cosmic strings exhibit a Doppler peak of acceptable height in small angle anisotropies.[7] The problem is that it is difficult to estimate the anisotropy in the cosmic string model, including the simulations of the string network and the fluctuations of baryons and CDM. To add above reasons, there are reports of the non-

Gaussian aspects of cosmic microwave background radiation.[8] Therefore it seems that it is too early to exclude the cosmic string model and that it is still worthwhile to investigate this scheme further.

First we overview the treatment of the formation of astronomical objects in the cosmic string scheme. The main assumptions in our prototype model are:

A) There is one long and fast ($v \sim 0.7c$) cosmic string passing through the universe during each e-folds expansion, where v and c are the string velocity and the velocity of light, respectively. CDM accumulates toward the two-dimensional trace of the string and a wake is formed there.[9]

B) Astronomical objects are formed in the intersection of three wakes triggered at suitable epochs of redshift $z_{\rm i}$.

The assumption A) seems to be in disagreement with the numerical simulations of local gauge strings, which indicate the existence of several wiggly slow ($v \sim 0.15c$) strings in the universe.[10] However, numerical simulations show also that sometimes fast ($v > 0.7c$) strings pass through the universe.[11] From a purely observational point of view, it seems better to have one wake for each horizon scale.[12]

With regard to the assumption B), we have made some numerical simulations of the formation and fragmentation of a wake triggered by a straight string with an appropriate density perturbation of the Harrison-Zeldovich (HZ) spectrum.[13] In general a CDM falling toward the wake tends to accumulate at nonlinear high-density sites. Therefore it is reasonable to assign the nonlinear high-density sites to the crossing regions of three wakes. In principle there exist many small wakes caused by the motion of cosmic strings in the early universe.

In the following, typical objects are described by $z_{\rm i}$, which means that they are formed at intersecting sites of three wakes triggered by strings at, e.g., $z_{\rm i} \times e$, $z_{\rm i}$ and $z_{\rm i}/e$. Different trigger times of $z_{\rm i}$ are adopted for simplicity to describe the resultant hierarchical structure of the astronomical objects distinctly. The objects with $z_{\rm i}$ should therefore be interpreted as representing also the objects with neighboring values of $z_{\rm i}$. The basic features of the formation of astronomical objects in this scheme are CDM accumulations toward the nonlinear high density sites such as the crossing points of three wakes and the behavior of the baryonic matter around and within them attracted by the CDM gravity.

The main point which we would like to show is that the hierarchical structure of astronomical objects can be explained using this cosmic string scheme. For instance, objects with $z_{\rm i} \simeq 10^4$, 10^5 and 10^6 become objects corresponding to clusters of galaxies, galaxies and dwarf galaxies, respectively.

In this scheme, smaller objects gradually accumulate toward larger objects hierarchically. That is, at the present time most dwarf galaxies have already accumulated into galaxies, and galaxies are still now accumulating toward clusters of galaxies. The nuclei of accumulated dwarf galaxies would be found as some of the globular clusters in galaxies, and many of the accumulated galaxies are found as E and/or SO galaxies in clusters of galaxies. In the future (or possibly at present) clusters of galaxies will accumulate toward super-clusters (objects with $z_{\rm i} \simeq 10^3$ in this scheme).

It is approximated in this paper that the objects triggered at $z_{\rm i}$ have become objects of the same mass and radius. The number density of these objects $n(z_{\rm i})$ is

related to horizon size $l(z_{\rm i}, z)$ as $n(z_{\rm i}) \propto 1/l(z_{\rm i}, z)^3$ (see Eqs. (13) and (14) below). In this paper the probability distribution function is not considered in detail. The distribution function is investigated further for objects formed at $z_{\rm i} \simeq 10^4$ and compared with the observation in Ref. 14), where the distribution of string velocities and the effects of tilted angles among three crossing wakes are considered. In principle, it would be better to include such a probability function for each stage of $z_{\rm i}$ to compare with the observation. However, this complicates the situation greatly and we believe that it is better to present the framework of this scheme simply and clearly for the moment.

In §2 we investigate the reionization of the universe in this scheme taking into account heating due to the release of the gravitational energy of inwardly falling matter. The hierarchical structure of the universe is comprehensively investigated in §3. Other problems such as the evolution into galaxies and clusters of galaxies are discussed in §4. Throughout this paper we assume a flat universe with baryonic and CDM densities $\Omega_b \simeq 0.05$ and $\Omega_d \simeq 0.95$ and use the value of Hubble constant $H_0 = 50\ {\rm km\,s^{-1}\ Mpc^{-1}}$.

§2. Reionization of the universe

2.1. *Giant HII regions*

The mass and radius of CDM accumulated at the crossing site of three wakes evolve with redshift as [15)]

$$M \simeq M_0(G\mu\beta\gamma/3\times10^{-6})^3/[(1+z)/(1+z_{\rm sat})]^3 \tag{1}$$

and

$$R \simeq R_0(G\mu\beta\gamma/3\times10^{-6})/[(1+z)/(1+z_{\rm sat})]^2, \tag{2}$$

where μ and β are the line density and the velocity of cosmic string in units of $c = 1$, γ being $(1-\beta^2)^{-1/2}$. In the above equations, the application is limited for $1+z \geq 1+z_{\rm sat}$. This limiting condition results from the fact that almost all CDM within the horizon at $z_{\rm i}$ has completed its infall toward the crossing site of three wakes at $z \simeq z_{\rm sat}$.[4), 15)] The values of M_0, R_0, $1+z_{\rm sat}$, L_0 (see Eq. (3a)), T_0 (Eq. (3b)), the horizon size (Eq. (14)), the number density (Eq. (13)) and other characteristic values of the objects with various $z_{\rm i}$ are presented in Table I.

As gas falls deeply into the CDM potential, the gas motion is slowed down by thermal pressure and/or shock waves. For simplicity we consider here only heating by the dissipative release of kinetic energy of inwardly falling gas in the CDM potential.

The heating rate and the corresponding gas temperature at redshift z are estimated to be

$$\begin{aligned} L_{\rm heat} &\simeq \Omega_b dM/dt \times v^2/2 \simeq \Omega_b dM/dt \times GM/(f_R \times R) = L_0[(1+z)/(1+z_{\rm sat})]^{-5/2} \\ &\simeq 0.1 \times (\Omega_b/0.05) GM_0^2 f_c/\{t_0 R_0[(1+z)/(1+z_{\rm sat})]^{5/2}\} \end{aligned} \tag{3a}$$

and

$$T \simeq 2/3 \times GMm_{\rm H}/(k_{\rm B} f_R \times R) = T_0[(1+z)/(1+z_{\rm sat})]^{-1}$$

Table I. Characteristic values for crossing sites of three wakes. The characteristic mass, radius, dispersion velocity ($f_R = 1$), saturation stage, horizon scale at present, number density (adopting $f_{\rm ob} = 0.1$), collapsed stage, z_c, when the Jeans instability begins, heating luminosity and temperature at $1+z_{\rm sat}$ (present value for the case of $1+z_{\rm sat} < 1$) are presented for various values of $1+z_{\rm i}$. The asterisk (*) indicates the saturation stage in the future (*$1/n$ represents the stage of n times expansion of the universe from now). The corresponding present day astronomical objects are indicated for them. With regard to the supercluster, the horizon size should be noted for its scale, and the values of the mass and radius are understood to be the values for the central core of the supercluster.

$1+z_{\rm i}$	M_0 ($\rm M_\odot$)	R_0 (pc)	v ($\rm km\,s^{-1}$)	$1+z_{\rm sat}$	Horizon (pc)	$n_{\rm ob}$ ($\rm Mpc^{-3}$)
10^7	3.8×10^6	6.8×10^2	6.7	6.7	4.7×10^4	9.7×10^2
3×10^6	1.4×10^8	2.7×10^3	21	5.4	1.5×10^5	2.7×10^1
10^6	3.7×10^9	1.1×10^4	54	4.1	4.6×10^5	1.0
3×10^5	1.4×10^{11}	5.2×10^4	150	2.9	1.5×10^6	2.7×10^{-2}
10^5	3.5×10^{12}	2.5×10^5	350	1.8	4.6×10^6	1.0×10^{-3}
3×10^4	8.6×10^{13}	1.3×10^6	760	*0.8	1.5×10^7	3.1×10^{-5}
10^4	1.3×10^{14}	1.5×10^6	870	*1/3	4.1×10^7	1.5×10^{-6}
3×10^3	8.1×10^{13}	1.3×10^6	740	*1/10	1.1×10^8	6.8×10^{-8}
10^3	2.6×10^{13}	8.6×10^5	510	*1/30	2.6×10^8	6.0×10^{-9}

$1+z_{\rm i}$	$1+z_c$	L_0 ($\rm erg\,s^{-1}$)	T_0 (K)	Astronomical objects
10^7	6	7.2×10^{33}	2.0×10^3	dwarf galaxies (lower limit)
3×10^6	33	1.6×10^{36}	1.7×10^4	dwarf galaxies (small)
10^6	77	2.0×10^{38}	1.2×10^5	dwarf galaxies
3×10^5	126	3.2×10^{40}	9.2×10^5	galaxies (small)
10^5	220	2.4×10^{42}	5.1×10^6	galaxies (large)
3×10^4	313	1.1×10^{44}	2.4×10^7	groups of galaxies
10^4	316	2.3×10^{44}	3.1×10^7	clusters of galaxies
3×10^3	238	9.8×10^{43}	2.3×10^7	superclusters of galaxies
10^3	153	1.5×10^{43}	1.1×10^7	superclusters of galaxies

$$\simeq 2/3\times GM_0 m_{\rm H} f_c/\{k_{\rm B}R_0\times[(1+z)/(1+z_{\rm sat})]\}, \tag{3b}$$

where $t = t_0/(1+z)^{3/2}$, $k_{\rm B}$ and $m_{\rm H}$ are the age of the universe at redshift z ($t_0 = 4.7\times10^{17}$ s), the Boltzmann constant and the mass of hydrogen atom. Here the inwardly falling gas is assumed to stop at radius $f_R R$. As the density distribution of CDM is $\rho \propto r^{-3/2}$, the radial dependence of CDM mass [10] is $M(r) \propto r^{3/2}$. Therefore we could estimate the temperature of the inwardly falling gas assuming that the gas is stopped at $f_R R$. The temperature is proportional to $(3-2\sqrt{f_R})GM/R$, because the potential at r ($= f_R R$) is $V(r) = f_c GM/R$ with $f_c = (3-2\sqrt{f_R})$ ($1 \le f_c \le 3$). For objects with $z_{\rm i} = 10^4$, 10^5 and 10^6, the heating rate and the temperature thus estimated take the following values (see Table I).

$z_{\rm i} = 10^4$:

$$L_{\rm heat} \simeq 2.3\times10^{44} f_c (M_0/1.3\times10^{14}\ \rm M_\odot)^2 (R_0/1.5\ Mpc)^{-1}(1+z)^{-5/2}\ erg\,s^{-1}, \tag{4a}$$

$$T \simeq 3.1\times10^7 f_c (M_0/1.3\times10^{14}\ \rm M_\odot)(R_0/1.5\ Mpc)^{-1}(1+z)^{-1}\ K. \tag{4b}$$

$z_{\rm i} = 10^5,\ 1+z > 1.8\ (z_{\rm sat} \simeq 0.8)$:

$$L_{\rm heat} \simeq 2.4 \times 10^{42} f_c (M_0/3.5 \times 10^{12}\ {\rm M}_\odot)^2 (R_0/0.25\ {\rm Mpc})^{-1} \times [(1+z)/1.8]^{-5/2}\ {\rm erg\,s^{-1}}, \tag{5a}$$

$$T \simeq 5.1 \times 10^6 f_c (M_0/3.5 \times 10^{12}\ {\rm M}_\odot)(R_0/0.25\ {\rm Mpc})^{-1}[(1+z)/1.8]^{-1}\ {\rm K}. \tag{5b}$$

$z_{\rm i} = 10^6,\ 1+z > 4.1\ (z_{\rm sat} \simeq 3.1)$:

$$L_{\rm heat} \simeq 2.0 \times 10^{38} f_c (M_0/3.7 \times 10^{9}\ {\rm M}_\odot)^2 (R_0/1.1 \times 10^{-2}\ {\rm Mpc})^{-1} \times [(1+z)/4.1]^{-5/2}\ {\rm erg\,s^{-1}}, \tag{6a}$$

$$T \simeq 1.2 \times 10^5 f_c (M_0/3.7 \times 10^{9}\ {\rm M}_\odot)(R_0/1.1 \times 10^{-2}\ {\rm Mpc})^{-1}[(1+z)/4.1]^{-1}\ {\rm K}. \tag{6b}$$

The values for objects with $z_{\rm i} \simeq 10^4$ are the representative values for X-ray observed clusters of galaxies.[16] The comparison of these values with observations is given in §3.

It must be checked whether the heating rate $L_{\rm heat} \simeq \Omega_b dM/dt \times v^2/2$ is less than the cooling rate due to bremmstrahlung which is given for the objects with $z_{\rm i} = 10^4$, 10^5 and 10^6 by

$$\begin{aligned} L_{\rm brem} &\simeq 1.8 \times 10^{-27} n_{\rm e}^2 T^{0.5} (4\pi (f_R R)^3), \\ &\simeq 1.4 \times 10^{42} (M_0/1.3 \times 10^{14}\ {\rm M}_\odot)^{5/2} f_c^{1/2} f_R^{-7} (R_0/1.5\ {\rm Mpc})^{-7/2} \\ &\quad \times (1+z)^{5/2} (\Omega_b/0.05)^2\ {\rm erg\,s^{-1}}, \\ &\simeq 3.8 \times 10^{41} (M_0/3.5 \times 10^{12}\ {\rm M}_\odot)^{5/2} f_c^{1/2} f_R^{-7} (R_0/0.25\ {\rm Mpc})^{-7/2} \\ &\quad \times [(1+z)/1.8)]^{5/2} (\Omega_b/0.05)^2\ {\rm erg\,s^{-1}}, \end{aligned} \tag{7}$$

and

$$\begin{aligned} &\simeq 5.1 \times 10^{39} (M_0/3.7 \times 10^{9}\ {\rm M}_\odot)^{5/2} f_c^{1/2} f_R^{-7} (R_0/1.1 \times 10^{-2}\ {\rm Mpc})^{-7/2} \\ &\quad \times [(1+z)/4.1)]^{5/2} (\Omega_b/0.05)^2\ {\rm erg\,s^{-1}}, \end{aligned}$$

respectively. For objects with $z_{\rm i} = 10^4$ and 10^5, the condition $L_{\rm brem} \geq L_{\rm heat}$ is satisfied if $f_R \leq 0.3$ and 0.8, respectively. However, even in the case of $L_{\rm brem} \leq L_{\rm heat}$, the intracluster medium will later become inhomogeneous, and the cooling rate would exceed $L_{\rm heat}$ due to the high density regions. This picture suggests that cooling flow will occur in a certain number of clusters of galaxies and that the matter falling inward at the early stage is gaseous (in the later stage, some fraction of baryons will change to stars that are today E, SO or spirals). Therefore the baryon to CDM ratio would increase towards the center.[17),18)]

For objects with $z_{\rm i} = 10^6$, the temperature cited in Table I (see also Eq. (6b)) seems to be insufficiently high to ionize the hydrogen. However, if $f_c \geq 2$ ($f_R \leq 0.25$), the temperature becomes high enough to ionize the hydrogen before $z \simeq 7$. But, if we consider that other heating sources, such as O, B stars, supernovae and/or X-rays from compact objects, have ionized the surrounding medium, the potential with $z_{\rm i} = 10^6$ is not deep enough to bound the heated ionized gas. It is thus inferred that objects with $z_{\rm i} = 10^6$ have been in a state close to self-regulating star formation within the shallow potential. This could explain the characteristics of dwarf galaxies for their long history of star formation and low surface brightness.[19] As there remains a large uncertainty in the heating rate by such sources, we continue to investigate the gas ionization around objects by assuming the heating rate to be $\Omega_b dM/dt \times v^2/2$, where f_c is a factor including the uncertainty.

The radius of the HII region is estimated from the balance between ionization and recombination as $R_{\rm HII} \simeq (3N_{\rm uv}/4\pi n_{\rm e} n_{\rm H} \alpha^{(2)})^{1/3}$, where $\alpha^{(2)}$ ($= 2 \times 10^{-13} (T/10^4\ {\rm K})^{-1/2}\ {\rm cm^3\ s^{-1}}$), $n_{\rm e}$, $n_{\rm H}$ and $N_{\rm uv}$ are the recombination rate of hydrogen,[20] the number densities of electrons and ionized hydrogens ($n_{\rm e} \simeq n_{\rm H}$) and the UV photon emission rate from the central star, respectively. Then the radius of the HII region is

$$R_{\rm HII} \simeq 5 \times 10^7 (M_0/1.3 \times 10^{14}\ {\rm M_\odot})^{1/3} (1+z)^{-5/2}\ {\rm pc}, \tag{8}$$

where the relation $N_{\rm uv} \simeq L/k_{\rm B}T \simeq (3\Omega_b/m_{\rm H}) dM/dt$ has been used. Setting $R_{\rm HII}$ equal to half the horizon (Eq. (14) below) with $z_{\rm i} \simeq 10^4$ or 10^5, it follows that the ionization of the universe by objects with $z_{\rm i} \simeq 10^4$ or 10^5 has completed at $1+z \simeq 3.6$ or $1+z \simeq 7.7$, respectively. Here we have assumed the equilibrium between recombination and ionization. However, the equilibrium condition is not applicable after $1+z \sim 20$, because the equality of the recombination time $t_{\rm recomb} \simeq 1/(n_{\rm H}\alpha^{(1)})$, where $\alpha^{(1)} \simeq 1.6 \times \alpha^{(2)}$ at $T = 10^4$ K,[20] with the expansion time of the universe $t_{\rm exp} = t_0/(1+z)^{3/2}$ yields

$$1 + z \simeq 19.2 (T/10^4\ {\rm K})^{1/3} (\Omega_b/0.05)^{-2/9}. \tag{9}$$

After the above-mentioned stage ($1+z \leq 20$), recombination could be neglected in the outer homogeneous medium for $t_{\rm recomb} > t_{\rm exp}$. Then the ionization front should be identified by the radius of the ionized region. The ionizing radiation energy integrated up to redshift z is given by

$$L_{\rm tot} = \int L dt = 3\Omega_b f_c G M_0^2/(4R_0(1+z)^4), \tag{10}$$

and the radius of the HII region at z is estimated as

$$R_{\rm HII}(z) \simeq (3L_{\rm tot}(z)/(4\pi n_{\rm H} h\nu)^{1/3}, \tag{11}$$

where $h\nu$ ($\simeq 13.6$ eV) is the ionization energy of hydrogen. Thus estimated values of $R_{\rm HII}$ for objects with $z_{\rm i} \simeq 10^4$, 10^5 and 10^6 are respectively

$$R_{\rm HII}(z) \simeq 4.6 \times 10^7 (M_0/1.3 \times 10^{14}\ {\rm M_\odot})^{2/3} (R_0/1.5 \times 10^6\ {\rm pc})^{-1/3} f_c^{1/3} \times (1+z)^{-7/3}\ {\rm pc}, \tag{12a}$$

$$\simeq 4.2\times 10^6 (M_0/3.5\times 10^{12}\ \mathrm{M}_\odot)^{2/3}(R_0/2.5\times 10^5\ \mathrm{pc})^{-1/3} f_c^{1/3} \times ((1+z)/1.8)^{-7/3}\ \mathrm{pc}, \tag{12b}$$

and

$$\simeq 2.2\times 10^5 (M_0/3.7\times 10^9\ \mathrm{M}_\odot)^{2/3}(R_0/1.1\times 10^4\ \mathrm{pc})^{-1/3} f_c^{1/3}((1+z)/4.1)^{-7/3}\ \mathrm{pc}. \tag{12c}$$

2.2. *Reionization of the universe*

As the number ratio of the objects with $z_\mathrm{i} = 10^4$, 10^5 and 10^6 in this scheme [15] is $1 : 10^3 : 10^6$, the ratio of their contribution to the heating of the universe is $1 : 60 : 39$ at the stage $z \simeq 3.1$ as seen by considering Eqs. (4a), (5a) and (6a). Since the ionization energy of the hydrogen is 13.6 eV, the contribution of objects with $z_\mathrm{i} = 10^6$ to the reionization of the universe seems to be smaller than the value estimated above. For objects with $z_\mathrm{i} = 10^4$ and 10^5, the ionization began at $z \simeq 200$ and 60, respectively (the ionization of helium began at $z \simeq 50$ and 15, respectively).

We consider the reionization stage to be the epoch when the emitted energy equals the ionization energy of total amount of neutral hydrogen within the mean separation length of objects with z_i, $l_\mathrm{ml}(z_\mathrm{i}) \simeq [n_\mathrm{ob}(z_\mathrm{i})]^{-1/3}$. Here the number density $n_\mathrm{ob}(z_\mathrm{i})$ of the objects of z_i is assumed to be given by

$$n_\mathrm{ob}(z_\mathrm{i}) = f_\mathrm{ob}/l(z_\mathrm{i}, z)^3, \tag{13}$$

where f_ob is a factor determined from observations and $l(z_\mathrm{i}, z)$ is the horizon length of the universe at z_i observed at z, given by [4]

$$l(z_\mathrm{i}, z) = 155[1 + ((1+z_\mathrm{eq})/(1+z_\mathrm{i}))^{1/2}]^{-1}(1+z)^{-1} h_{50}^{-1}\ \mathrm{Mpc}, \tag{14}$$

where z_eq ($\sim 6\times 10^3$) is the redshift of the epoch when radiation and matter densities were equal. The number density of luminous clusters of galaxies in X-ray and optical observations yields $f_\mathrm{ob} \sim 10^{-1}$ ($n_\mathrm{ob} \simeq f_\mathrm{ob}(l(z_\mathrm{i} = 10^4, 0))^{-3} \simeq f_\mathrm{ob} \times 10^{-6}\ \mathrm{Mpc}^{-3}$, whereas in X-ray observation [16), 21)] this is $n_\mathrm{ob}(L_\mathrm{X} \geq 10^{44}\ \mathrm{erg\,s^{-1}}) \simeq 3\times 10^{-7}\ \mathrm{Mpc}^{-3}$, and in optical observation, [22)] $n_\mathrm{ob}(M \geq 10^{14}\ \mathrm{M}_\odot) \simeq 10^{-7}\ \mathrm{Mpc}^{-3}$).

Then the energy needed to complete the ionization within the mean separation length is

$$L_\mathrm{ion} = n_\mathrm{H}(z)[l_\mathrm{ml}(z_\mathrm{i})]^3 h\nu. \tag{15}$$

From the condition $L_\mathrm{tot} \geq L_\mathrm{ion}$, the reionization stage can be estimated as $1 + z \simeq (1+z_\mathrm{sat})((3\Omega_b f_c G M_0^2/4R_0)/L_\mathrm{ion})^{1/4} \simeq 2.2\times((f_c/3)f_\mathrm{ob})^{1/4}$, $4.9\times((f_c/3)f_\mathrm{ob})^{1/4}$ and $4.5\times((f_c/3)f_\mathrm{ob})^{1/4}$ for objects with $z_\mathrm{i} = 10^4$, 10^5 and 10^6, respectively. If we adopt the value $f_\mathrm{ob} \sim 10^{-1}$, the reionization stage becomes too late, because QSO observations show that the universe is reionized at least before $z \simeq 5$ (Gunn-Peterson Effect). [23)]

Since we have neglected heating by compact objects, such as active galactic nuclei (supermassive black holes), X-ray binaries and UV luminous massive stars, the above estimates suggest that the contribution by these objects must be also taken into account (see, e.g. Ref. 24)). If this is true, what kind of objects had contributed

most to the reionization of the universe? The heating rate will be proportional to the mass accreted into the parent objects with $z_{\rm i} \simeq 10^4 - 10^6$, because the heating from compact objects must be proportional to the number of such compact objects, which must be proportional to the accreted mass. The ratio of the accumulated mass to the background mass for each generation is proportional to $f_{\rm ob} \times ((1+z_{\rm sat})/(1+z))^3$, because $M = M_0((1+z_{\rm sat})/(1+z))^3$. Then objects with $z_{\rm i} = 10^6$ (dwarf galaxies) must be dominant before $z = 0.8$ (see Table I). However, as indicated by Silk, Wyse and Shields,[19] several supernovae could disperse the interstellar gas of dwarf galaxies. Thus it is difficult to estimate precisely the contribution of objects with $z_{\rm i} \simeq 10^6$ to the ionization of the universe.

Finally, the energy needed for the reionization of the horizon scale with $z_{\rm i} \simeq 10^4$ (~ 40 Mpc at present) is estimated to be

$$E_{\rm rei} \simeq \Omega_b \times (40\ {\rm Mpc})^3 \times (\rho_c/m_{\rm H}) \times h\nu \simeq 6 \times 10^{60}\ {\rm erg} \simeq 3.5 \times 10^6\ {\rm M}_\odot c^2, \quad (16)$$

where ρ_c is the critical density of the universe at present. This implies that a consumption of rest mass energy amounting to $3.5 \times 10^6\ {\rm M}_\odot c^2$ is needed for the reionization of the horizon scale with $z_{\rm i} \simeq 10^4$. From the QSO observations, there is a lower bound for the comoving number density ($17.5\, h_{50}^{-3}\, {\rm Gpc}^{-3}$) of luminous QSOs ($M_{\rm B} \leq -26$; $L \geq 8 \times 10^{46}\ {\rm erg\,s^{-1}}$) at $z \simeq 4.3$.[25] If such QSOs radiate at the Eddington critical luminosity, the QSO black hole mass must be $M \geq 6 \times 10^7\ {\rm M}_\odot$. Taking the radiative efficiency of the accreted mass to be 0.1, the integrated energy emitted by such a quasar is of the order of $6 \times 10^6\ {\rm M}_\odot c^2$. However, this is not sufficient for the reionization of the universe because of its scarcity ($\sim 10^{-3}/(40\ {\rm Mpc})^3$). This estimate is used to derive the lower bound. Some other observations seem to be within the same order of magnitude as the lower bound.[26] Therefore we conclude that at least the most luminous quasars are not the main energy source of the reionization of the universe. From these facts that the reflection model of AGN X-rays may be able to explain the cosmic X-ray background as well as the UV flux required to explain the properties of QSO absorption lines.[24]

§3. Hierarchical structure of astronomical objects

In the following we describe the characteristic features of objects with $z_{\rm i} = 10^4$, 10^5, 10^6, 10^7 and 10^3, respectively. It is interesting that they seem to correspond to the observed hierarchical structure of astronomical objects. The relations among their mass, radius, velocity dispersion and X-ray luminosity are also investigated from this point of view.

As noted in the Introduction, we have made the approximation that objects triggered at $z_{\rm i}$ become objects of the same mass and radius. In reality there is some distribution of mass and radius. If we include such a probability distribution function, the derived results would become much more complicated, and it would be difficult to understand the process and formation of the hierarchical structure clearly. It seems better to adopt simplifying assumptions to present the framework of this scheme for the moment.

3.1. *Typical generations in hierarchical structure*

3.1.1. Objects with $z_{\rm i} = 10^4$

The mass, radius and number density of CDM objects with $z_{\rm i} = 10^4$ obtained from the simulation in our scheme [15] and by Eqs. (1), (2) and (13) are given in Table I. The density distribution [15] of CDM is

$$\rho(r) \simeq 10^{-16}(r/0.1\ \mathrm{pc})^{-3/2}\,\mathrm{g\,cm^{-3}}. \quad (0.1\ \mathrm{pc} < r < 1.5\ \mathrm{Mpc}) \tag{17}$$

These are comparable to the observed characteristic values of clusters of galaxies. Density distributions with the power-law dependence $\rho \propto r^{-3/2}$ in the outer region are inferred from X-ray observations. [27] Moreover, the observed X-ray luminosity could be explained by this scheme (see §3 II-d). The interpretation is that clusters of galaxies are still accumulating dark matter as well as baryonic matter. At present some fraction of inwardly falling matter would be in the form of objects with $z_{\rm i} \simeq 10^5 - 10^6$, corresponding to galaxies and/or dwarf galaxies which would retain diffuse gas components. [18] It is also noted that clusters are not so fully virialized (at least for galaxies) as commonly believed, especially in the outer region.

The horizon radius at $z_{\rm i} = 10^4$ expanded up to the present is $\sim 40(a/a_0)/2$ Mpc, and the accumulating radius is $\sim 1.5(a/a_0)^2 \times 3\sqrt{3}$ Mpc, where a is the expansion parameter (scale factor) of the universe, having the present value a_0. Therefore the mass accretion to clusters of galaxies will continue more than three expansion times ($a/a_0 \simeq 3$) from now on until it completes.

The mass function, correlation function and other features of clusters of galaxies are also explained in this model. [14),28] It naturally follows that the brightest cluster members such as gE, D and cD galaxies exist at the cluster center. [29]

3.1.2. Objects with $z_{\rm i} = 10^5$

The simulated mass and radius of CDM objects with $z_{\rm i} = 10^5$ are given by Eqs. (1), (2) and in Table I. The density distribution [15] of CDM is

$$\rho(r) \simeq 10^{-15}(r/0.01\ \mathrm{pc})^{-3/2}\,\mathrm{g\,cm^{-3}}. \quad (0.01\ \mathrm{pc} < r < 2.5 \times 10^2\ \mathrm{kpc}) \tag{18}$$

The number density is also given in Table I. These are comparable with characteristic values for galaxies. As mentioned above, the accumulation of dark matter toward such objects has been completed at $z \simeq 0.8$. Hence it may not be so common for such objects to be luminous in X-rays. Although they may emit a great quantity in X-rays before $z \simeq 0.8$, when dark and baryonic matter accrete on these crossing points, today the X-ray bright generation has shifted from galaxies to clusters of galaxies on the whole. (However, objects with $z_{\rm i} \simeq 10^4$ have been most luminous.) We discuss X-ray luminosities (§3 II-d) and the evolution of these objects into galaxies (§4 I) below.

3.1.3. Objects with $z_{\rm i} = 10^6$

The mass, radius and number density for objects with $z_{\rm i} = 10^6$ are given in Table I. The density distribution [15] of CDM is

$$\rho(r) \simeq 10^{-12}(r/10^{-4}\ \mathrm{pc})^{-3/2}\,\mathrm{g\,cm^{-3}}. \quad (10^{-4}\ \mathrm{pc} < r < 10\ \mathrm{kpc}) \tag{19}$$

Although there are not so many observations about dwarf galaxies, the derived values are not so much different from the characteristic ones of dwarf galaxies. The accumulation of CDM toward such objects was completed at $z \simeq 3.1$. There could be an extension of the period of star formation [30] if gas is not completely removed from dwarf galaxies by X-rays or UV heating from nearby objects with $z_{\rm i} \simeq 10^4 - 10^5$. Also, if they exist close to objects with $z_{\rm i} = 10^5$, the heating from them may suppress the formation of stars in the outer envelope of dwarf galaxies. [30]

In addition, most of them must have already accumulated toward galaxies, because the observed mass fraction of dwarf galaxies is very small compared to galaxies in the low galaxy density field and local groups of galaxies. [31),32] As stated above, the extended envelopes of dwarf galaxies are suppressed if they are located near the parent galaxy. When dwarf galaxies accreted into galaxies, their extended envelopes, if they existed, were destroyed by tidal interaction with the parent galaxy [33] and other inwardly falling objects, and their central parts would remain as some globular clusters as fossils of accreted dwarf galaxies. Such a view of the origin of globular clusters arising from captured dEn galaxies has been proposed by Freeman [34] as the Searle-Zinn picture. [35]

In the high galaxy density region (e.g. Coma cluster and Virgo cluster), the mass fraction of dwarf galaxies seems not to be small. [30] They are accreted not only into galaxies but also into the larger gravitational potential with $z_{\rm i} = 10^4$. Thus many dwarf galaxies will remain and could be found there.

3.1.4. Objects with $z_{\rm i} = 10^7$

The mass, radius and number density of CDM for objects with $z_{\rm i} = 10^7$ are given in Table I. The density distribution of CDM is

$$\rho(r) \simeq 10^{-12}(r/10^{-6}\ {\rm pc})^{-3/2}\,{\rm g\,cm^{-3}}. \quad (10^{-6}\ {\rm pc} < r < 6.8 \times 10^2\ {\rm pc}) \qquad (20)$$

These values seem to be comparable to characteristic quantities for globular clusters, but there is not enough matter for the Jeans instability to grow within their potentials before $z \geq 6$. Therefore the above values should be taken as the lower limits of the mass and radius for a single luminous object (smallest dwarf irregular galaxies). The lowest observed mass of dwarf galaxies is $3 \times 10^6\ {\rm M}_\odot$, [32] which is very close to the mass of objects with $z_{\rm i} \simeq 10^7$. However, there remains the possibility that stellar systems will be formed therein, because the shock waves propagate from nearby objects with $z_{\rm i} \simeq 10^3 - 10^6$. In any case most of the smallest dwarf irregular galaxies must have accreted into dwarf or normal galaxies.

As described above, at the present time clusters of galaxies are accumulating galaxies observed as E or SO galaxies there, while these galaxies have previously accumulated dwarf galaxies, and the dwarf galaxies have accumulated objects with $z_{\rm i} = 10^7$. Such dark matter potentials causing the formation of hierarchical structure, [15] if they are not disrupted, could perhaps be observed in the future using sophisticated telescopes (8 and 10 m-telescopes with good CCD-cameras and adaptive optics) and techniques.

3.1.5. Objects with $z_{\rm i} = 10^3$

Finally, the mass, radius and number density for objects with $z_{\rm i} = 10^3$ are given in Table I. The density distribution of CDM is

$$\rho(r) \simeq 10^{-19}(r/0.86\ {\rm Mpc})^{-3/2}\,{\rm g\,cm^{-3}}. \quad (1\ {\rm pc} < r < 0.86\ {\rm Mpc}) \tag{21}$$

The number density of such objects is 10^{-3} times that of rich clusters of galaxies. Thus these objects will rarely be observed. However they will gradually capture clusters of galaxies in the future until 30 times expansion of the present universe.[15] Their mass and radius will finally reach $M \sim 7 \times 10^{17}\ {\rm M}_\odot$ and $R \sim 800$ Mpc. It is difficult to consider that objects with $z_{\rm i} \simeq 10^3$ will be accumulated toward objects with $z_{\rm i} \simeq 10^2$ and so on, because the universe becomes very inhomogeneous after $z \simeq 10^2$ and the inhomogeneity of CDM suppresses the wake formation (with $z_{\rm i} \leq 10^2$).[13]

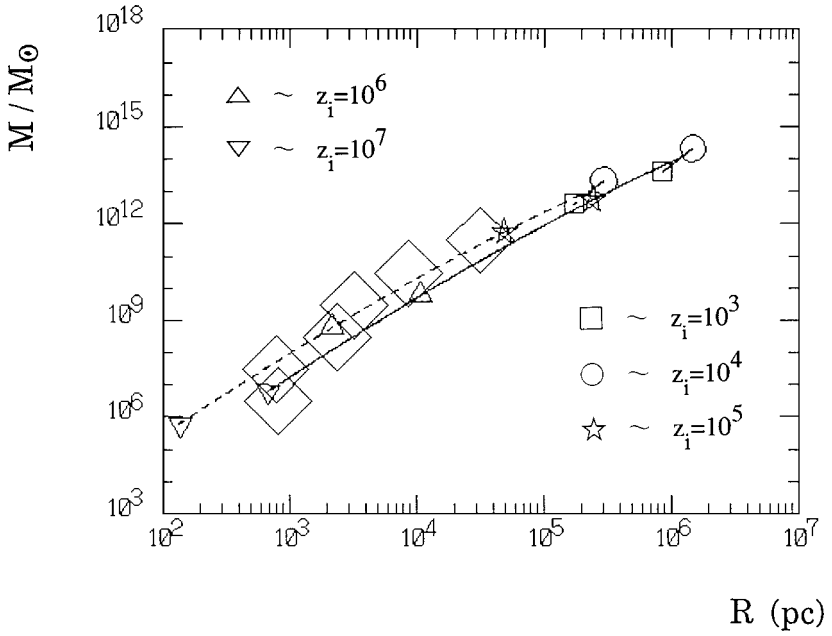

Fig. 1. Mass vs radius for objects with $z_{\rm i} \simeq 10^3 - 10^7$. The relation between the present mass (M) and radius (R) for objects with $z_{\rm i} \simeq 10^3 - 10^7$ is described by the solid curve. The case of $M_{\rm lum} = f_M M$ and $R_{\rm lum} = f_R R$ with $f_M = 0.1$ and $f_R = 0.2$ is indicated by the dashed curve. Objects with $z_{\rm i} = 10^3$, 10^4, 10^5, 10^6 and 10^7 are denoted by squares, circles, stars, triangles and inverse triangles, respectively (on the solid and dashed curves). The observed values for galaxies and dwarf galaxies in nearby ($\leq 10^2$ Mpc) local groups[33] are indicated by large diamonds. Their radii are determined with the arithmetic mean for all mass in the range $10^n - 10^{n+1}\ {\rm M}_\odot$ with $n = 6$, 7, 8, 9 and 10 and the corresponding mass is taken as $\sqrt{10} \times 10^n\ {\rm M}_\odot$, respectively.

3.2. *Correlations among characteristic values of formed objects*

3.2.1. Mass vs radius

The mass-radius (M-R) relation for objects with $z_{\rm i} \simeq 10^3 - 10^7$ are displayed by the solid curve in Fig. 1, where objects with $z_{\rm i} = 10^3$, 10^4, 10^5, 10^6 and 10^7 are denoted by the small squares, circles, stars, triangles and inverse triangles, respectively (on the solid curve). The observed values for galaxies and dwarf galaxies are obtained from nearby local groups ($\leq 10^2$ Mpc) [32] and denoted by large diamonds in each order of mass scale. If we consider that gas has contracted and formed luminous objects within the CDM potential, the observed results should be compared with $M_{\rm lum} = f_M M$ and $R_{\rm lum} = f_R R$, introducing the fractional factors f_M and f_R. The relation between $M_{\rm lum}$ and $R_{\rm lum}$ with $f_M = 0.1$ and $f_R = 0.2$ is represented by the dashed curve in Fig. 1, where the corresponding objects with $z_{\rm i} = 10^3$, 10^4, 10^5, 10^6 and 10^7 are indicated by the same symbols as for CDM objects (on the long dashed curve). With this correction, the M-R relation comes to agree better with the observation in the mass range $10^9 - 10^{12}$ $M_\odot$. However, in the mass range $10^6 - 10^9$ $M_\odot$, luminous objects seem to be distributed extensively within the dark matter potential. This may be due to the shallow potentials of these objects.

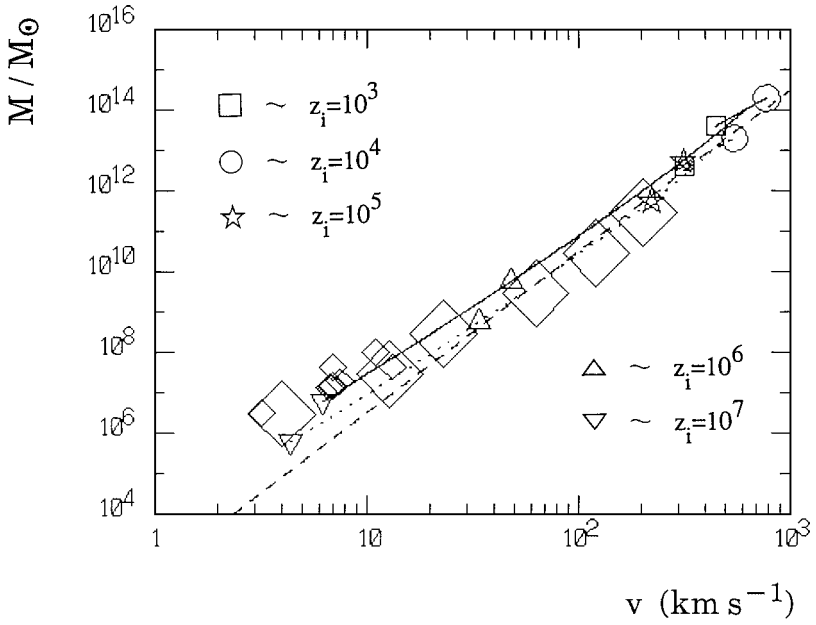

Fig. 2. Mass vs dispersion velocity for objects with $z_{\rm i} \simeq 10^3 - 10^7$. The relation between the mass and dispersion velocity is represented by solid curve. The case of $M_{\rm lum}$ and $R_{\rm lum}$ with $f_M = 0.1$ and $f_R = 0.2$ is indicated by the dotted curve. The Tully-Fisher relation, $L(\propto M) \propto v^4$, is represented by the long dashed line with the normalization $v = 200$ km s^{-1} at 10^{12} $M_\odot$. Other symbols are the same as in Fig. 1. Small diamonds represent the observations of the Galactic dwarf spheroids. [34]

3.2.2. Mass vs dispersion velocity

The relation of the mass and dispersion velocity ($v = (2f_cGM/R)^{1/2}$ with $f_c = 1$) is represented in Fig. 2 by the solid curve. The case of $M_{\rm lum}$ and $R_{\rm lum}$ with $f_M = 0.1$ and $f_R = 0.2$ is represented by the dotted curve. Assuming that the luminosity is proportional to the mass and that the rotation velocity v_R is related to the dispersion velocity v as $v = \sqrt{2}v_R$, the Tully-Fisher relation $L \propto v_R^4$ ($\propto M$) is obtained. This is represented by the long dashed line[36] with the normalization $v = 200$ km s^{-1} at 10^{12} M$_\odot$. The observed values for nearby local groups are denoted by large diamonds.[32] Other symbols, such as squares, circles, stars, triangles and inverse triangles, are the same as in Fig. 1. The small diamonds represent the observation of the Galactic dwarf spheroids.[33] The relation $v_R^4 \propto M$ holds almost exactly in the range $10^8 \leq M/\ {\rm M}_\odot \leq 10^{14}$.

3.2.3. Radius vs dispersion velocity

The simulated relation between the radius R and the dispersion velocity v is represented by the solid curve in Fig. 3. The case of $f_M = 0.1$ and $f_R = 0.2$ is represented by the dotted curve. The observed relation[37] $R \propto v^{1.45}$ is described by the long dashed line with the normalization $v = 10^2$ km s^{-1} at $R = 10$ kpc. The predicted relation in this scheme seems to be correlated to the observation at around $10 - 10^2$ km s^{-1}.

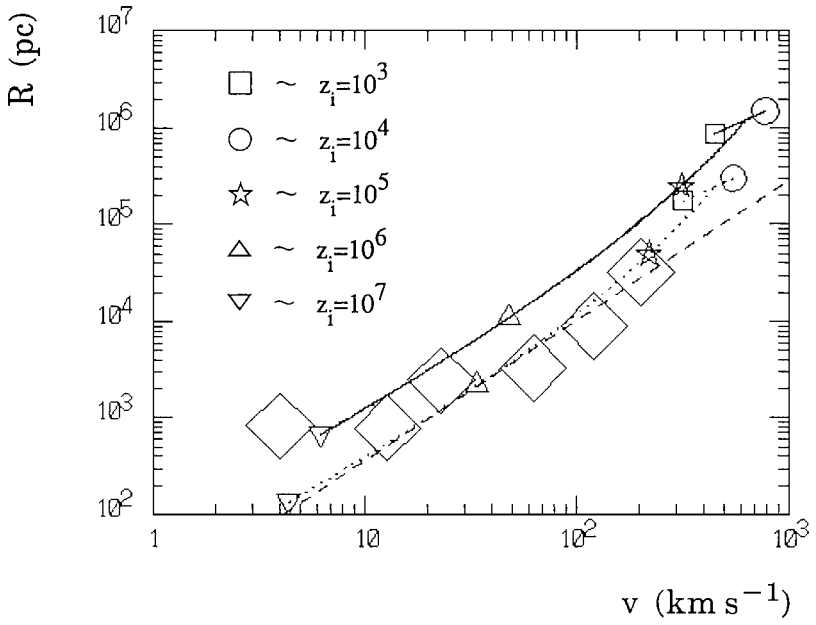

Fig. 3. Radius vs dispersion velocity for objects with $z_{\rm i} \simeq 10^3 - 10^7$. The relation between the radius and dispersion velocity is represented by the solid curve. The case of $M_{\rm lum}$ and $R_{\rm lum}$ with $f_M = 0.1$ and $f_R = 0.2$ is indicated by the dotted curve. The observed values for nearby local groups are indicated by large diamonds. The observed relation $R \propto v^{1.45}$ is represented by the long dashed line with the normalization $v = 10^2$ km s^{-1} at $R = 10$ kpc.

3.2.4. X-ray luminosity vs dispersion velocity

We present the X-ray luminosity vs dispersion velocity in Fig. 4. The X-ray luminosity is taken from Eq. (3a) and the dispersion velocity is estimated by $v = (2f_cGM/R)^{1/2}$, where we take $f_R = 0.2$ ($f_c = 3 - 2\sqrt{f_R} \simeq 2$). The long dashed line represents the X-ray luminosity at its maximum (at $z = z_{\rm sat}$ for each $z_{\rm i}$ object and $z = 0$ if $1 + z_{\rm sat} < 1$). Then we have to include the decay factor from the maximum luminosity, because after $z \simeq z_{\rm sat}$ the X-ray luminosity would decay due to the decrease and/or the exhaustion of inwardly falling matter. Although it is difficult to estimate $L_{\rm x}$ after $z = z_{\rm sat}$, we estimate it by assuming an exponential decay as

$$L_{\rm x} = L_0 \times \exp(-c_{\rm decay}(t_0 - t_{\rm sat})/t_{\rm sat}), \tag{22}$$

where t_0 and $t_{\rm sat} = t_0/(1 + z_{\rm sat})^{3/2}$ are the present and the age of the universe at $z = z_{\rm sat}$, respectively. The solid line depicts the case for $c_{\rm decay} = 1$, taking into account that the cooling time for hot interstellar medium is of the order of $t_{\rm sat}$ corresponding to $z_{\rm sat}$.

The observed X-ray luminosities [38] and velocity dispersions [39] for clusters of galaxies are indicated by the diamonds. The dotted line indicates the observed correlation between $L_{\rm x}$ and v ($L_{\rm x} \simeq 4.2 \times 10^{44}(v/10^3\ {\rm km\,s^{-1}})^4$) for clusters of galaxies. [16] The observed X-ray luminosities for early-type galaxies are plotted by the

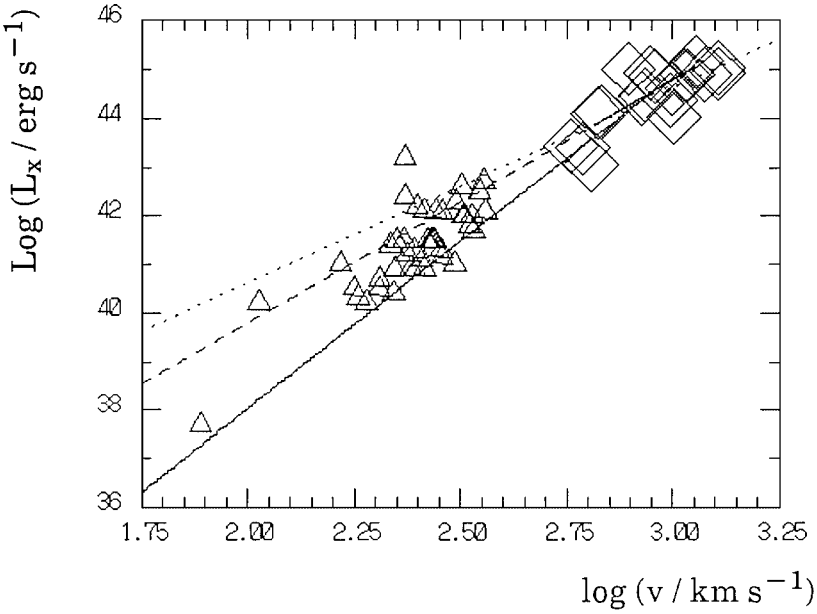

Fig. 4. X-ray luminosity vs dispersion velocity for objects with $z_{\rm i} \simeq 10^3 - 10^7$. X-ray luminosity of Eq. (7) and the dispersion velocity with $f_R = 0.2$ is given by the solid line. Equation (3a) with $f_R = 0.2$ at $z = z_{\rm sat}$ ($z = 0$ for $1 + z_{\rm sat} < 1$) is plotted by the long dashed line. The observed X-ray luminosities [38] and velocity dispersions [39] for clusters of galaxies are indicated by diamonds. The dotted line represents the relation $L_{\rm x} \simeq 4.2 \times 10^{44}(v/10^3\ {\rm km\,s^{-1}})^4$ obtained for clusters of galaxies. [16] The observed X-ray luminosities for early-type galaxies are plotted by triangles. [40] The lower left one is NGC221.

triangles.[40] The lower left one is NGC221. It has been noted that $L_{\rm x}$ is dominated by discrete sources for early-type galaxies.[40),41] As we use $L_{\rm x}$ for the diffuse component, the solid line should be taken as the indicator of the lower limit for early-type galaxies.

Even though there are simplified assumptions, this scheme could explain the characteristic observed X-ray properties of clusters of galaxies and early-type galaxies.

§4. Discussion

4.1. *Evolution into galaxies*

The mass and radius of accumulating objects increase with time as shown by Eqs. (1) and (2). The typical values of objects with $z_{\rm i} = 10^5$ are presented in Table II at $z = 10,\ 8,\ 6,\ 4,\ 2,\ 0.8$ and 0, respectively. One should note that the increase in the mass and radius of galaxies is very rapid after $z \simeq 4$, and especially after $z \simeq 2$. The mass and radius of inwardly falling objects at each stage (objects with $z \simeq z_{\rm sat}$) are also given there by asterisks (*). Also, the mass and radius of inwardly falling objects increase with time. Moreover, there must be relatively homogeneous components of falling matter. Objects with $z_{\rm i} \simeq 10^5$ seem to correspond to bright or giant galaxies. From the observed rotation velocity $v_R \simeq v$, objects with $z_{\rm i} \simeq 3 \times 10^5$ seem to correspond to small galaxies (see Table I). Then normal spirals of $v_R \simeq 200\ {\rm km\,s^{-1}}$ seem to correspond to objects with $10^5 < z_{\rm i} < 3 \times 10^5$. Even though heated up by the X-rays from the parent object, the inwardly falling objects and CDM may retain some fraction of baryonic gas components. If the configuration is non-spherical due to differences in the strength of wakes and/or crossing angles of three wakes, the accumulated baryons eventually tend to form a disk when sufficiently cooled. However the stellar components of the inwardly falling objects would linger about the center and form a stellar halo.

If the central parts of inwardly falling objects are not destroyed by the tidal

Table II. Evolution into galaxies for objects with $z_{\rm i} \simeq 10^5$ at various stage. The characteristic CDM mass and radius of object with $z_{\rm i} \simeq 10^5$ at various stages represented by z are presented. The fractions of mass and radius of accumulated objects at each stage compared with the final values are estimated by $[(1+z)/(1+z_{\rm sat})]^{-3}$ and $[(1+z)/(1+z_{\rm sat})]^{-2}$, respectively. The luminous part should be taken to be within $R_{\rm lum} = f_R R$ ($f_R \simeq 0.1-0.2$) and $M_{\rm lum} = f_M M$ ($f_R \simeq 0.05-0.1$). The asterisk (*) indicates the typical mass and radius of inwardly falling objects at each stage z.

z	$\left[\frac{(1+z)}{(1+z_{\rm sat})}\right]^{-3}$	M ($\rm M_\odot$)	$\left[\frac{(1+z)}{(1+z_{\rm sat})}\right]^{-2}$	R (kpc)	M*($\rm M_\odot$)	R* (pc)
10	0.4%	1.5×10^{10}	3%	6.7	~ 10	~ 10
8	0.8%	2.8×10^{10}	5%	13	$\sim 10^3$	$\sim 10^2$
6	1.7%	6.0×10^{10}	9%	23	$\sim 3 \times 10^6$	$\sim 7 \times 10^2$
4	4.7%	1.6×10^{11}	13%	32	$\sim 10^8$	$\sim 3 \times 10^3$
2	22%	7.6×10^{11}	36%	90	$\sim 4 \times 10^9$	$\sim 10^4$
0.8	100%	3.5×10^{12}	100%	250	$\sim 10^{11}$	$\sim 5 \times 10^4$
0	100%	3.5×10^{12}	100%	250		

force of parent object, they will survive to be found as some globular clusters. The difference in the number of globular clusters between E and S type galaxies may be due to the difference in the geometrical configuration of CDM potentials to destroy the inwardly falling objects by tidal forces.[42] During such tidal interactions with the parent object and/or interaction with neighboring inwardly falling objects, star bursts may occur in the inwardly falling objects.

For S-type galaxies, the disk component is stable if there is no accretion of large mass components in the last several Gyr. From this scheme, objects with $z_{\rm i} \simeq 10^5$ and 3×10^5 are considered to have almost ceased the accumulation of inwardly falling objects after $z \simeq 1$ and 2, respectively. On the other hand, this scheme indicates also that disk components are formed after $z \simeq z_{\rm sat}$, due to the decrease of heating by falling objects. After $z \simeq z_{\rm sat}$, a gaseous (geometrically) thick disk would be cooled down to become a geometrically thin disk.

The main part of the bulge component would be formed through a self-regulated star formation out of a low angular momentum gas cloud before $z \simeq z_{\rm sat}$. However, even after $z \simeq z_{\rm sat}$ some fraction of gas is thrust into the bulge through angular momentum transfer, and stars are formed there.

The size and mass of objects with $z_{\rm i} \simeq 10^5$ and 3×10^5 have almost completed growth at $z \simeq 1$ and 2, respectively. Then the number of these objects have been almost conserved over the last several Gyr. However, the number of lower mass galaxies (subgalaxies and/or dwarf galaxies) has decreased greatly before $z \simeq 1-2$ due to the accumulation to larger galaxies. If they accumulate into a cluster of galaxies (an object with $z_{\rm i} \simeq 10^4$), dwarf galaxies could survive there due to a much larger and extended dark matter potential (corresponding to a weak tidal force). This would explain the differences in the number ratio of E, S, dE and dSp for different environments.[31]

The mass range of dwarf galaxies extends to $10^6 - 10^{11}$ $M_\odot$. Even though the mean number density of these objects is greater than galaxies of $M \simeq 10^{12}$ $M_\odot$, the mass fraction of these objects will be much less than galaxies.[32] Therefore we have to assume that most dwarf galaxies have been inevitably accreted into galaxies, except in clusters of galaxies. The violent clustering (or accumulation) of objects with $z_{\rm i} \simeq 10^6 - 10^{11}$ to objects with $z_{\rm i} \simeq 10^5$ has occurred during $z \simeq 6 - 1$.

From the preliminary estimate in this scheme, the violent accretion of dwarf galaxies into large systems with $z_{\rm i} \simeq 10^5$ is complete at present. At the present time galaxies are moving into clusters of galaxies. However, there will be no star bursts, because baryons have almost all changed to stars in objects with $z_{\rm i} \geq 10^5$. The mass fraction of the interstellar medium is a few % in our galaxy, which may be a typical value for spiral galaxies. Although the transition of diffuse baryons to stars must have occurred violently in galaxies before $z \simeq 1$ and later become stationary, the fraction of the diffuse baryonic component in intergalactic space to total baryons is not well known. Inferring from the ratio of the gas mass to the stellar mass in clusters of galaxies, the fraction would still be considered[43] to be of order 1.

Table III. Evolution into clusters of galaxies for objects with $z_{\rm i} \simeq 10^4$. The same as Table II except for objects with $z_{\rm i} \simeq 10^4$.

z	$(1+z)^{-3}$	$M/\ {\rm M}_\odot$	$(1+z)^{-2}$	R (kpc)	$M^*/\ {\rm M}_\odot$	R^* (pc)
10	$7.5\times10^{-2}\%$	9.8×10^{10}	0.8%	12.	~ 10	~ 10
6	0.3%	3.8×10^{11}	1.2%	19	$\sim 3\times10^{6}$	$\sim 7\times10^{2}$
4	0.8%	1.0×10^{12}	4.0%	60	$\sim 10^{8}$	$\sim 3\times10^{3}$
2	3.7%	4.8×10^{12}	11%	170	$\sim 4\times10^{9}$	$\sim 10^{4}$
1	13%	1.6×10^{13}	25%	380	$\sim 10^{11}$	$\sim 5\times10^{4}$
0.5	30%	3.9×10^{13}	44%	670	$\sim 10^{12}$	$\sim 10^{5}$
0	100%	1.3×10^{14}	100%	1500	$\sim 3\times10^{12}$	$\sim 5\times10^{5}$

4.2. *Evolution to cluster of galaxies*

The typical physical values of objects with $z_{\rm i} = 10^4$ at $z = 10,\ 6,\ 4,\ 2,\ 1,\ 0.5$ and 0 are presented in Table III to trace the evolution of clusters of galaxies. The mass and radius of inwardly falling objects at each stage are also indicated there by asterisks (*). The increase in mass and radius of clusters [44] is very rapid after $z \simeq 1$ and/or 0.5. Therefore the evolution of clusters could be detected by observations, and indeed the evolutions of X-ray luminosities and the morphology of cluster galaxies are suggested by observations. [44), 45]

A dependence of the morphology of galaxies on the distance from cluster center has been observed in rich clusters of galaxies. [46] There could be two mechanisms to generate such a morphological difference. One is the difference in the formation epoch. Under this scheme it could be inferred as following. The early-type galaxies are formed early, due to the great strength of wakes and a symmetrical configuration. On the other hand, the strength of wakes for late type galaxies is not strong compared with early-type galaxies. Then the completion of CDM falling toward galaxies will be delayed for an asymmetrical configuration and/or weak strength of the wake. If we consider this possibility, the formation epoch of spiral galaxies must be delayed after $z \simeq 2$ and/or $\simeq 1$, especially for the disk components.

The second mechanism is the depletion of interstellar gas from galaxies by the high density intracluster medium (ICM). The evolution of disk components is suppressed and the conversion of spiral types to SO types may occur through tidal interaction with parent object and other neighboring galaxies. [44] This effect could be inferred from any formation scheme. Perhaps both mechanisms will reproduce the morphological difference with the distance from cluster center.

From the gas to star ratio $R_{\rm g\text{-}s}$ in clusters, where $R_{\rm g\text{-}s}$ ranges about from 1 to 6, and the chemical abundance of ICM, which is about $20-40\%$ of the solar abundance. Such a fraction of the ICM must have been the interstellar medium of galaxies (or dwarf galaxies). [43] There is a possibility to explain those observations in this scheme, because gas has passed through small objects with $10^4 < z_{\rm i} < 10^7$.

4.3. *Clustering and accretion*

There should be a gravitational interaction among objects with $z_{\rm i} \simeq 10^3 - 10^7$, which is usually called clustering. Tidal interactions and merging among those objects have been observed, however, the accretion of smaller objects into larger

objects (at the present time galaxies are accreted into clusters of galaxies) also should not be neglected. This accretion determines a CDM distribution of the form $\rho \propto r^{-3/2}$ around the formed object. The cosmic string scenario seems to be similar to the standard CDM scheme in some aspects. However, the main difference is the accretion effect. As stated above, clustering phenomena occur even in the cosmic string scheme. Gravitational interactions among objects of the same $z_{\rm i}$ should be considered clustering beyond the horizon scale of $z_{\rm i}$. However there is a tendency for them to accrete into larger objects. It seems that there is no such object with $z_{\rm i} \simeq 10^4$ in nearby groups of galaxies. Then the interaction among local groups of galaxies could be considered as clustering. Although it is difficult to determine whether the interactions are caused by clustering or accretion, it seems more difficult to derive the observed density distribution around formed objects through clustering than through accretion.

§5. Conclusions

Although details must be studied more closely, this simple model, where three wake crossings are triggered by cosmic strings, could explain the hierarchical structure of clusters of galaxies, galaxies and dwarf galaxies. The interesting point is that smaller objects (triggered earlier because of high $z_{\rm i}$, however Jeans instability occurred there later [15] because of small CDM potentials) have completed their formation earlier because of relatively large $z_{\rm sat}$ and accumulated into larger objects later. For example, dwarf galaxies are accreted into galaxies and observed as some globular clusters (This process is already mostly completed.) and galaxies are accreted into clusters of galaxies (This process is still proceeding.). This scheme predicts the accumulation of clusters of galaxies toward superclusters of galaxies (This process seems to become noticeable just recently.), and it has already been indicated by observations. [47), 28)]

The characteristic values of these objects, such as mass, radius and density distribution, can be explained in this scheme by taking a suitable value of one parameter, $G\mu\beta\gamma$. Even though the estimates are made on very simple assumptions, it is interesting to note that the obtained results are not very different from observations. Considering the accumulation of CDM and baryons into clusters of galaxies, their X-ray properties could also be explained. Heating by the release of gravitational energy when matter falls toward galaxies and clusters of galaxies is insufficient for the reionization of the universe before $z \simeq 5$. Therefore some other heating mechanism or active sources are required.

References

1) G. Blumenthal, S. Faber, J. Primack and M. Rees, Nature **311** (1984), 517.
S. D. White and C. S. Frenk, Astrophys. J. **379** (1991), 52.
S. Cole and C. Lacey, Mon. Not. R. Astron. Soc. **281** (1996), 99.
2) J. P. Ostriker, ARA & A, **31** (1993), 689.
M. White, D. Scott, J. Silk and M. Davis, Mon. Not. R. Astron. Soc. **276** (1995), L69.
J. F. Navarro, C. S. Frenk and S. D. M. White, Astrophys. J. **490** (1997), 493.

3) T. W. B. Kibble, J. of Phys. **A9** (1976), 1387.
A. Vilenkin, Phys. Lett. **C121** (1985), 263.
A. Vilenkin and E. P. S. Shellard, *Cosmic Strings and Other Topological Defects* (Cambridge Univ. Press, Cambridge, 1994).
H. Sato, Prog. Theor. Phys. **75** (1986), 1342.
4) T. Hara, P. Mähönen and S. Miyoshi, Astrophys. J. **412** (1993), 22.
5) U. Pen, U. Seljuk and N. Turok, Phys. Rev. Lett. **79** (1997), 1611.
6) N. Turok, Astrophys. J. **473** (1996), L5.
7) C. Contaldi, M. Hindmarsh and J. Magueijo, Phys. Rev. Lett. **82** (1999), 679.
8) P. Ferreira, J. Magueijo and K. M. Gorski, Astrophys. J. **503** (1998), L1.
L. Perivolaropoulos and N. S. Simatos, astro-ph/980321.
9) J. Silk and A. Vilenkin, Phys. Rev. Lett. **53** (1984), 1700.
M. J. Rees, Mon. Not. R. Astron. Soc. **222** (1986), 27p.
A. Stebbins, S. Veeraraghavan, R. Brandenberger, J. Silk and N. Turok, Astrophys. J. **322** (1987), 1.
T. Hara and S. Miyoshi, Prog. Theor. Phys. **77** (1987), 1152.
10) F. Bouchet and D. Bennett, Phys. Rev. **D41** (1990), 720.
B. Allen and E. P. S. Shellard, Phys. Rev. Lett. **64** (1990), 119.
A. Albrecht and N. Turok, Phys. Rev. Lett. **54** (1985), 1868.
11) E. P. S. Shellard and B. Allen, *The Formation and Evolution of Cosmic Strings* (Cambridge Univ. Press, Cambridge, 1990), p. 421.
12) T. Hara and S. Miyoshi, Astrophys. J. **405** (1993), 419.
13) T. Hara, P. Mähönen, H. Yamamoto and S. Miyoshi, Astrophys. J. **438** (1993), 27.
14) T. Hara, H. Yamamoto, P. Mähönen and S. Miyoshi, Astrophys. J. **432** (1994), 31.
15) T. Hara, H. Yamamoto, P. Mähönen and S. Miyoshi, Astrophys. J. **461** (1996), 1 .
16) C. Sarazin, Rev. Mod. Phys. **58** (1986), 1.
17) S. D. M. White, J. F. Navarro, A. E. Evrard and C. S. Frenk, Nature **366** (1993), 429.
18) N. Trentham, Nature **372** (1994), 157.
19) J. Silk, R. F. G. Wyse and G. A. Shields, Astrophys. J. **322** (1987), L59.
20) L. Spitzer, *Physical Process in the Interstellar Medium* (John Wiley & Sons, New York, 1978) .
21) R. Burg, R. Giacconi, W. Forman and C. Jones, Astrophys. J. **422** (1994), 37 .
22) N. A. Bahcall and R. Cen, Astrophys. J. **398** (1992), L81.
23) R. Jacobsen, A. Boksenberg, J. M. Dearveng, P. Greenfield, R. Jedrzejewski and F. Paresce, Nature **370** (1994), 35.
24) A. C. Fabian, I. M. Jeorge, S. Miyoshi and M. J. Rees, Mon. Not. R. Astron. Soc. **242** (1990), 14p.
25) E. L. Turner, Astron. J. **101** (1991), 5.
26) F. D. A. Hartwick and D. Schade, ARA & A **28** (1990), 437.
27) A. C. Fabian, *Clusters of Galaxies* (Frontiers, Singapore, 1994), p. 191.
S. Miyoshi, *Clusters of Galaxies* (Frontiers, Singapore, 1994), p. 187.
28) T. Hara, T. Matuura, H. Yamamoto, P. Mähönen and S. Miyoshi, Astrophys. J. **428** (1994), 51.
29) J. L. Tonry, *Structure and Dynamics of Elliptical Galaxies* (Reidel, Dordrecht, 1987), p. 89.
30) S. van den Bergh, Astrophys. J. **428** (1994), 617.
31) H. Jerjen, G. A. Tammann and B. Binggeli, *Morphological and Physical Classification of Galaxies* (Kluwer Acad., Dordrecht, 1992), p. 17.
32) I. Karachentsev, Astron. Astrophys. **305** (1996), 33.
33) M. Irwin and D. Hatzidimitrou, Mon. Not. R. Astron. Soc. **277** (1995), 1354.
34) K. C. Freeman, *The Globular Cluster-Galaxy Connection* (Astro. Soc. Pac. Con. Series, Vol. 48, San Francisco, 1993), p. 608.
35) L. Searle and R. Zinn, Astrophys. **225** (1978), 357.
36) W. van Driel, A. van den Broek and W. A. Baan, Astrophys. J. **444** (1995), 80.
37) I. Jorgensen, M. Franx and P. Kjaergaard, Astrophys. J. **411** (1993), 34.
38) A. C. Edge, G. C. Stewart and A. C. Fabian, Mon. Not. R. Astron. Soc. **258** (1992), 177.
39) M. Girardi, D. Fadda, G. Giuricin, F. Mardirossian and M. Mezzetti, Astrophys. J. **457** (1996), 61.

40) P. B. Eskridge, G. Fabbiano and D. Kim, Astrophys. J. Suppl. **97** (1995), 141.
P. B. Eskridge, G. Fabbiano and D. Kim, Astrophys. J. **442** (1995), 523.
41) L. Ciotti, A. D'Ercole, S. Pellegrini and A. Renzini, *Morphological and Physical Classification of Galaxies* (Kluwer Acad., Dordrecht, 1992), p. 179.
42) S. van den Bergh, Astrophys. J. **435** (1994), 203.
43) C. Jones and W. Forman, *Clusters and Superclusters of Galaxies* (Kluwer Acad., Dordrecht, 1992), p. 49.
44) A. Dressler, Jr., A. Oemler, W. B. Sparks and R. A. Lucas, Astrophys. J. **435** (1994), L23.
45) J. P. Henry, *Clusters and Superclusters of Galaxies* (Kluwer Acad., Dordrecht, 1992), p. 311.
46) A. Oemler, *Clusters and Superclusters of Galaxies* (Kluwer Acad., Dordrecht, 1992), p. 29.
47) M. Einasto, J. Einasto, E. Tago, G. B. Dalton and H. Andernach, Mon. Not. R. Astron. Soc. **269** (1994), 301.